

# Modeling laser brightness from cross Porro prism resonators

Andrew Forbes<sup>1#</sup>, Liesl Burger<sup>1</sup> and Igor Anatolievich Litvin<sup>1</sup>  
<sup>1</sup>CSIR National Laser Centre, PO Box 395, Pretoria 0001, South Africa

## ABSTRACT

Laser brightness is a parameter often used to compare high power laser beam delivery from various sources, and incorporates both the power contained in the particular mode, as well as the propagation of that mode through the beam quality factor,  $M^2$ . In this study a cross Porro prism resonator is considered; crossed Porro prism resonators have been known for some time, but until recently have not been modeled as a complete physical optics system that allows the modal output to be determined as a function of the rotation angle of the prisms. In this paper we consider the diffraction losses as a function of the prism rotation angle relative to one another, and combine this with the propagation of the specific modes to determine the laser output brightness as a function of the prism orientation.

**Keywords:** Porro prism resonators, laser brightness

## 1. INTRODUCTION

Right angle prisms, often referred to as Porro prisms, have the useful property that all incident rays on the prism are reflected back parallel to the initial propagation direction, independent of the angle of incidence. Thus an initial planar wavefront remains planar after reflection. This property was initially exploited in Michelson interferometers to relax the tolerances on mis-alignment, and then proposed in 1962 by Gould et al<sup>1</sup> as a means to overcome misalignment problems in optical resonators employing Fabry-Perot cavities, by replacing the end face mirrors with crossed roof prisms. Lasers based on this principle have been developed over the years<sup>2-6</sup> with a review of the basic concepts and literature for Porro prisms specifically found in [7]. Much of the theoretical work to date has focused on geometric methods to model the inverting properties of such resonators<sup>2-4</sup> and polarization considerations to account for internal phase shifts and output polarization states<sup>6,7</sup>. In [2] the prism was modeled as a ray deviator by replacing an imaginary mirror some distance behind the prism. The model correctly accounted for the beam direction, but did not account for the complex field distribution found experimentally from the laser. Even the physical optics models fail to account for the true field pattern found from such resonators<sup>3,8</sup>. In [3] for example, the kernel of the Fresnel-Kirchoff diffraction integral contains only the OPL experienced by the beam, thus treating the prism as though it were acting like a perfect mirror, with an identical ABCD matrix representation albeit incorporating the inverting properties of the prisms. This approach appears to be the preferred model for prisms<sup>7</sup>, even though it does not explain the complex transverse field patterns found in Porro prism resonators. This is a recurring problem in the literature, with only a hint at a solution offered in [8,9], where it is proposed to treat the field patterns as a result of diffractive coupling between a linear combination of sub-resonators. Anan'ev<sup>9</sup>, in considering the theoretical properties of resonators with corner cube prisms, specifically mentions the influence of bevels of finite width at the prism edges as a possible explanation for tendency for independent oscillation at different parts of the cross-section (looking down the length of the resonator), but does not go on to develop this idea into a model which can be used to explain experimental results. Recently<sup>10,11</sup> we have successfully shown that a physical optics approach to the prisms can be formulated that correctly predicts all the salient features of the transverse modal patterns observed from such resonators. With this model we are able, for the first time, to relate the properties of the laser beam to the modal patterns observed from such resonators. Using this approach, we apply the model to laser brightness, since this is the often used parameter for quantifying the energy delivery capability of a laser at some distance away (usually in the far field).

---

# [aforbes1@csir.co.za](mailto:aforbes1@csir.co.za); phone +27 12 8412368; fax +27 12 8413152

## 2. RESONATOR MODEL

The approach recently developed, which is summarized here but detailed fully elsewhere<sup>10,11</sup>, is to model a resonator containing crossed Porro prisms (Figure 1) as if the prisms are standard mirror elements, but with associated amplitude and phase screens. This deviates from approaches followed by others in the past in that it allows a complete physical optics model to be developed from this premise. In the case of a Porro prism, the amplitude screen introduces losses not only at the edges of the element, but also at the small but significant bevel where the prism surfaces meet. The phase screen allows for the optical path length to vary as a function of the input position on the prism face, for example, to model hanging roof edges or fabrication errors on the prism surfaces. With this approach, the diffractive effects of the prisms are taken into account, and the screens can be treated as intra-cavity elements that change the Eigenmodes of a standard mirror – mirror resonator. In this section we will only consider the effects of the amplitude screens on the modal patterns observed from such resonators (by assuming that the prism faces are perfect).

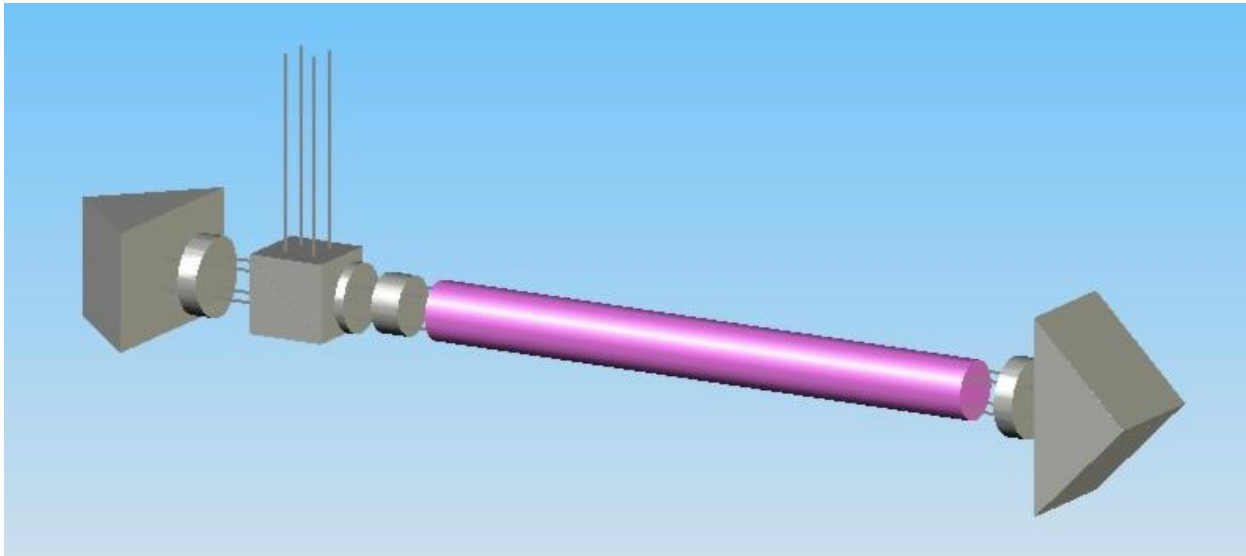


Figure 1: Illustration of the Porro prism resonator.

### 2.1 Symmetry and repeatability

In order to consider the symmetry and repeatability of the resonator modes, imagine that you observe the resonator along its length (i.e., looking down the length from one prism to the next), and that you could monitor the field as a 2 dimensional array perpendicular to this axis. We will assume, without any loss of generality, that the prism closest to the observer has an edge in the horizontal plane, and that the second prism is rotated at an angle of  $\pi/3$  relative to the first. We have *a priori* knowledge of how the mode will develop, and hence start with a beam location just in front of the first prism, as indicated in Figure 2a. After reflection from the back prism the beam is traveling towards the observer, and in a position inverted around the prism axis (Figure 2b). This beam is then inverted again about the front prism axis, as shown in Figure 2c. This process continues until the complete pattern is created (Figure 2f), and the beam has returned to its starting position, i.e., beam 7 repeats the same sequence starting from Figure 2a again. This argument can be applied to any arbitrary starting angle between the prisms, and similar patterns are generated for those angles that allow repeatability of the ray (some of which are shown in Figure 4). From a physical optics perspective, the same picture can be built up, but in this case it is not the ray that is rotating about the prism edges, but rather the lossy prism edges themselves that are inverted on each pass.

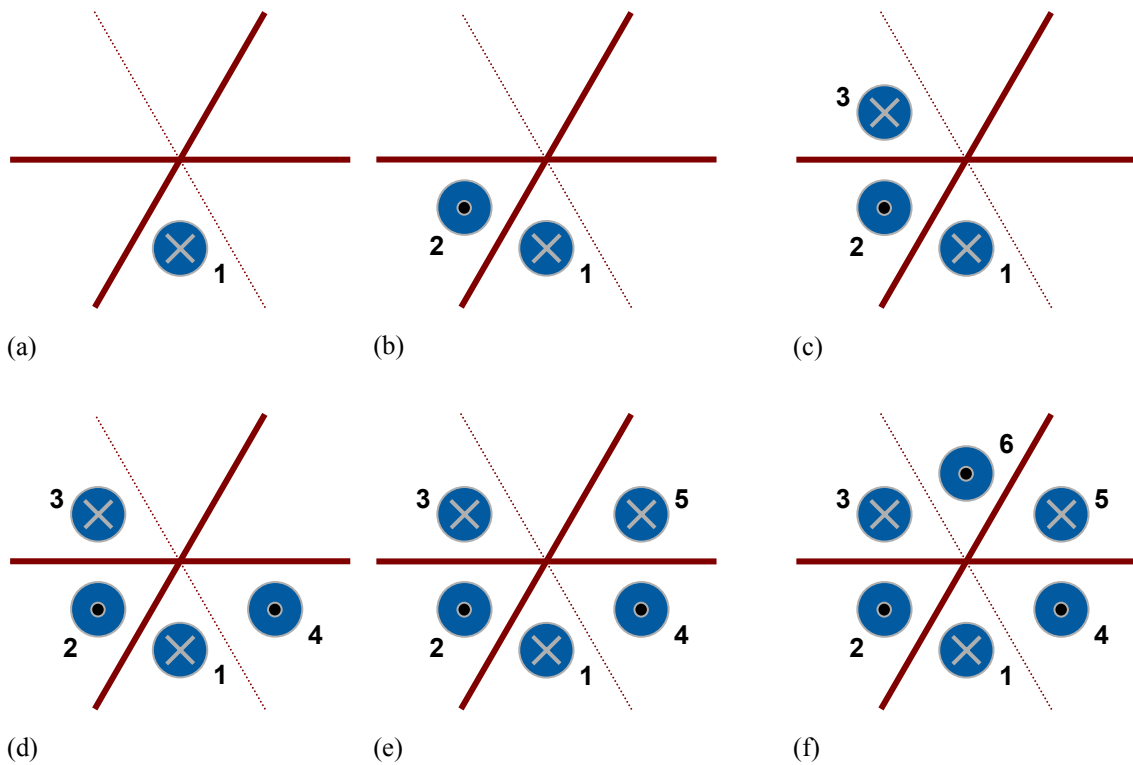


Figure 2: Looking down the resonator, along its length, with the nearest prism edge shown as the horizontal line. Starting with a ray in (a) moving towards the back prism, it is inverted and returns again as shown in (b). The return ray is then inverted off the front prism in (c) and the process repeats until after six passes (three round trips) the returning ray 6 (see (f)) returns onto ray 1 for the cycle to repeat.

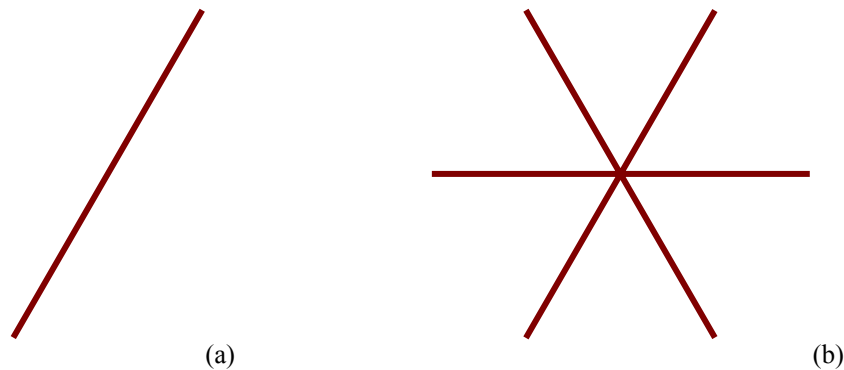


Figure 3: The physical optics equivalent of Figure 2. As a lossless field is reflected off the back prism, the edge introduces a loss across the field, as illustrated in (a) as a solid line. This lossy field is then inverted off the front prism, which does two things: (1) it introduces its own loss edge onto the field, and (2) it inverts the loss from the first prism to create an “additional” loss edge on the field, thus leaving the field with three loss edges, as shown in (b). This pattern will then repeat as the edges get inverted back on themselves.

One can shown from simple geometric arguments that the edges will start repeating on themselves after  $m$  passes if  $\pi - m\theta = 0$ , where  $m$  is the number of completed round trips. Also, since the inverting losses on the prism edges subdivide the field into two parts per pass, we will always have the condition that  $n = 2m$ , where  $n$  is the number of field sub-

divisions. These relationships lead to the following equation for the allowed angles of rotation of the prism edges relative to one another for repeatability after an integer number of round trips:

$$\theta = \frac{\pi}{m} = \frac{2\pi}{n} \tag{1}$$

### 2.2 Transverse mode patterns

This model was incorporated into a full resonator model of a crossed Porro prism resonator, and the effects on the transverse modal pattern investigated. The results are illustrated in Figure 4, where the stable prism angles are plotted with the corresponding number of expected “petals” due to the sub-division of the field. Note that Equation (1) gives rise to a discrete set of angles, which become closely packed as the integer  $m$  increases. Likewise, as  $m$  increases, the field becomes ever more sub-divided. Although this is possible from a purely theoretical point of view, at some stage (depending on the resonator parameters such as wavelength, size of the prisms, internal apertures etc) the subdivisions will simply be too small to allow lasing to occur.

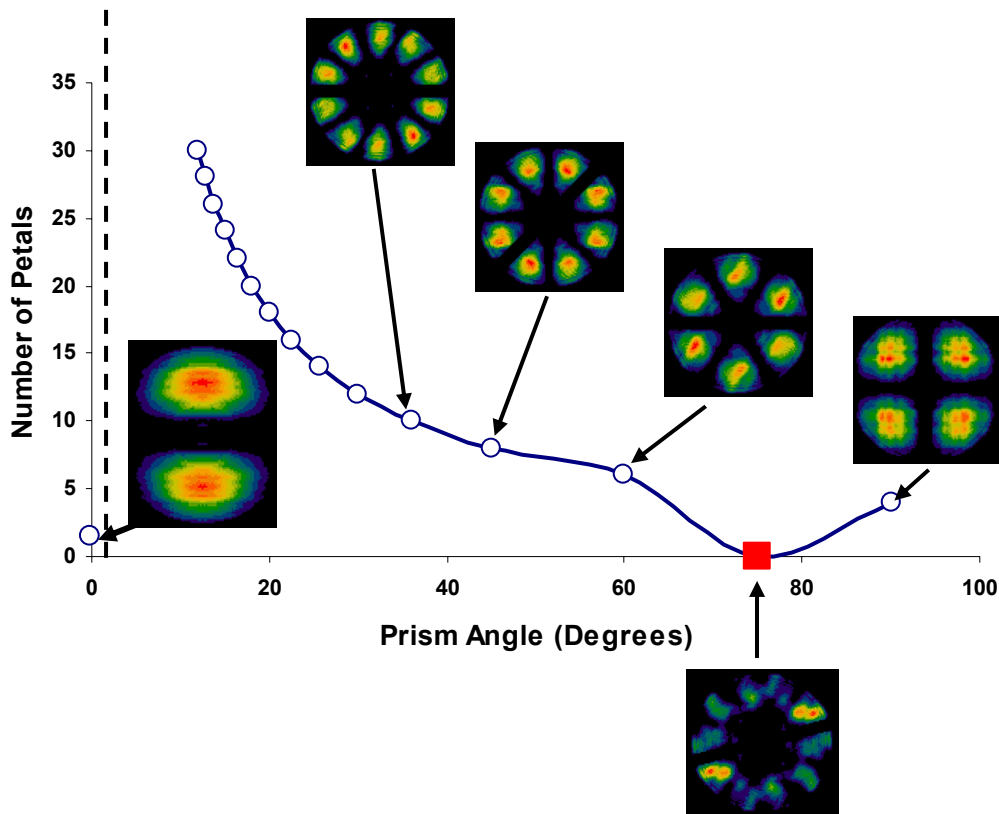


Figure 4: A plot showing at which prism angles the resonator will generate stable petal patterns with the corresponding number of expected petals. The graphic inserts are the numerically generated intensity profiles for the associated prism angles. The 75° data (solid square) is an angle for which no petal patterns should form, and is inserted here for comparative purposes only.

The above analysis gives rise to angles at which petals appear, and angles at which they don't. When they do appear, the angle also determines the number of petals generated, as well as how many round trips it takes for repeatability. Even without any analysis, it is obvious that factors such as the laser beam quality, output energy and laser brightness will also vary with prism angle, and this is what we investigate in the next section.

### 3. LASER BRIGHTNESS

Laser Brightness is a term often used in high energy laser delivery, or in systems for delivery of laser beams over very long distances (kilometer ranges). The value of this parameter is that it allows the output from various sources to be compared directly, regardless of the final delivery optics used.

#### 3.1 Basic definitions

The brightness of a light source is defined as the power (P) emitted per unit surface area (A), per unit solid angle ( $\Omega$ ):

$$B = \frac{P}{A\Omega}. \quad (2)$$

Following Siegman<sup>12</sup>, we define the quality of a laser beam using the  $M^2$  factor (laser beam quality factor), given as:

$$M_x^2 = \frac{4\pi\sigma_x\sigma_{sx}}{\lambda}. \quad (3)$$

Here  $\sigma_x$  is the second moment of the time averaged intensity profile of the laser beam  $I(x,y,z)$  and is given by the definition

$$\sigma_x^2(z) = \frac{\iint (x - \bar{x})^2 I(x, y, z) dx dy}{\iint I(x, y, z) dx dy}, \quad (4)$$

while the spatial frequency term,  $\sigma_{sx}$  is analogously the second moment of the spatial frequency distribution  $I_s(s_x, s_y, z)$

$$\sigma_{sx}^2(z) = \frac{\iint (s_x - \bar{s}_x)^2 I_s(s_x, s_y, z) ds_x ds_y}{\iint I_s(s_x, s_y, z) ds_x ds_y}. \quad (5)$$

Here we have defined all parameters in one transverse co-ordinate (x-transverse direction), but of course similar relations hold for the other transverse co-ordinate. In general the overall laser beam quality can be given as the product of the two co-ordinates, namely:

$$M^2 = M_x M_y. \quad (6)$$

For a circularly symmetric beam we may express the area of the laser beam as  $A = \pi\omega^2 = 4\pi\sigma^2$  and the solid angle as  $\Omega = \pi\theta^2 = 4\pi\sigma_s^2$ . If we now combine these definitions with Equation (2) and (3) we find

$$B = \frac{P}{M^4 \lambda^2}. \quad (7)$$

In general, for non-circularly symmetric beams, the laser brightness may be written as

$$B = \frac{P}{M_x^2 M_y^2 \lambda^2}. \quad (8)$$

Both Equations (7) and (8) can be interpreted in the same way: laser brightness increases if the power output from the laser increases, and if the beam quality from the resonator is enhanced. Both these parameters are resonator dependent, and thus we can expect that in the case of the Porro prism, where the mode pattern changes as the prisms are rotated, that the output brightness would also change.

### 3.2 Near and far field intensity distributions

A plot of the near field and far field second moment beam size is shown in Figure 5. It appears that for large prism angles the smaller number of petals gives rise to small second moments. This can be expected since the second moment method weights the contributions far from centroid very heavily. Thus more petals generate larger second moments.

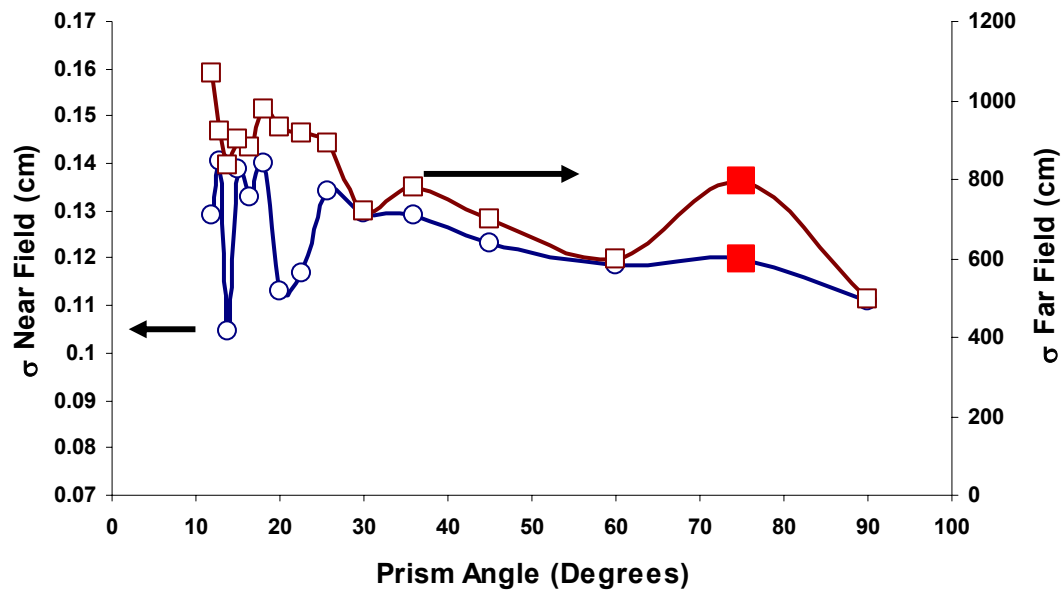


Figure 5: Plot of both near field and far field beam sizes for those angles at which petal patterns occur. The 75° data is included again for comparison.

A plot of the near field and far field intensity distributions is shown in Figure 6.

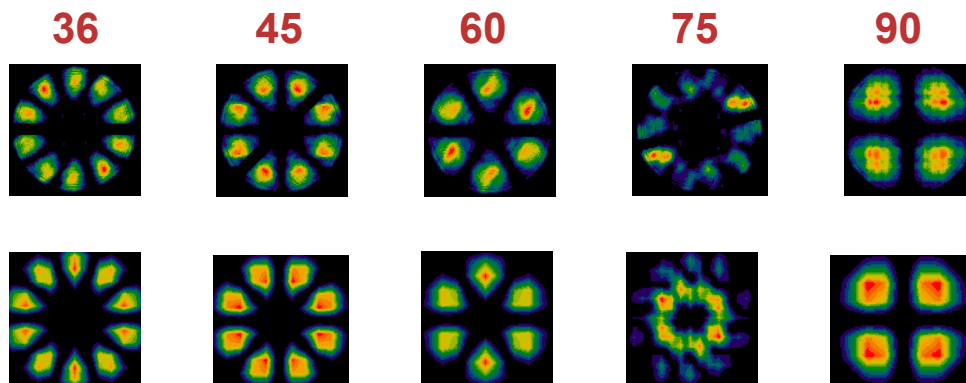


Figure 6: Plot of both near field (top row) and far field (bottom row) intensity distributions for 36°, 45°, 60°, 75° and 90°. The fact that the patterns hold their shape suggests that they make be treated as the sum of Gaussian fields. The 75° data is included again for comparison.

### 3.3 Laser beam quality ( $M^2$ )

The laser beam quality factor was calculated for all prism angles between  $0^\circ$  and  $90^\circ$ . As the number of petals decrease, so (generally speaking) the  $M^2$  factor also decreases, indicating that fewer petals correspond to an “improved” beam, as shown in Figure 7. The  $75^\circ$  data is again shown, and here it is clear that the  $M^2$  increases for non-petal pattern generating angles relative to those petal pattern generating angles near it.

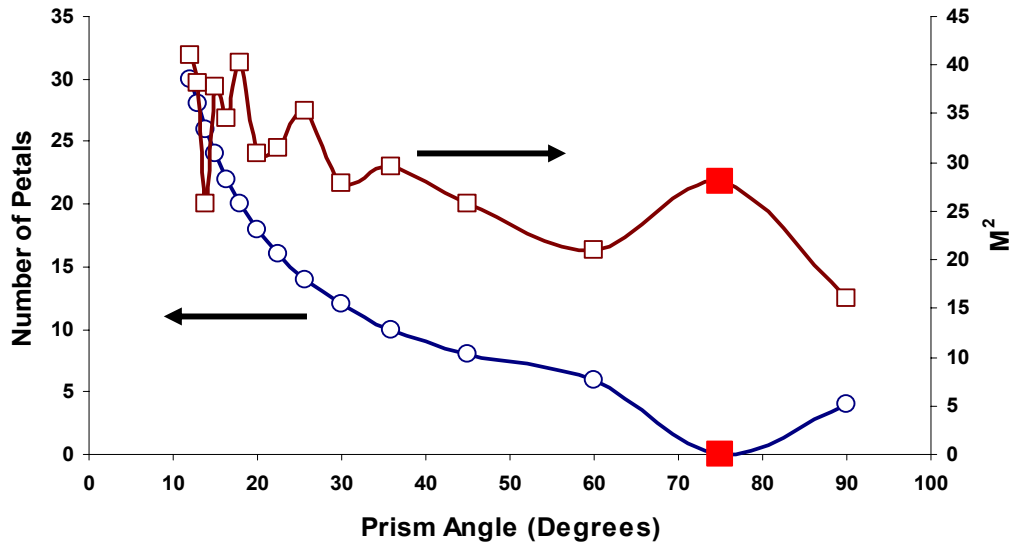


Figure 7: Beam quality factor for various those prism angles that generate repeating petal patterns.

### 3.4 Laser brightness

Finally, combining the results just shown we can generate a prediction of the laser brightness as a function of the prism angle. Figure 8 shows the normalized brightness plot ( $90^\circ$  data normalized to 1) for those angles which generate petal patterns.

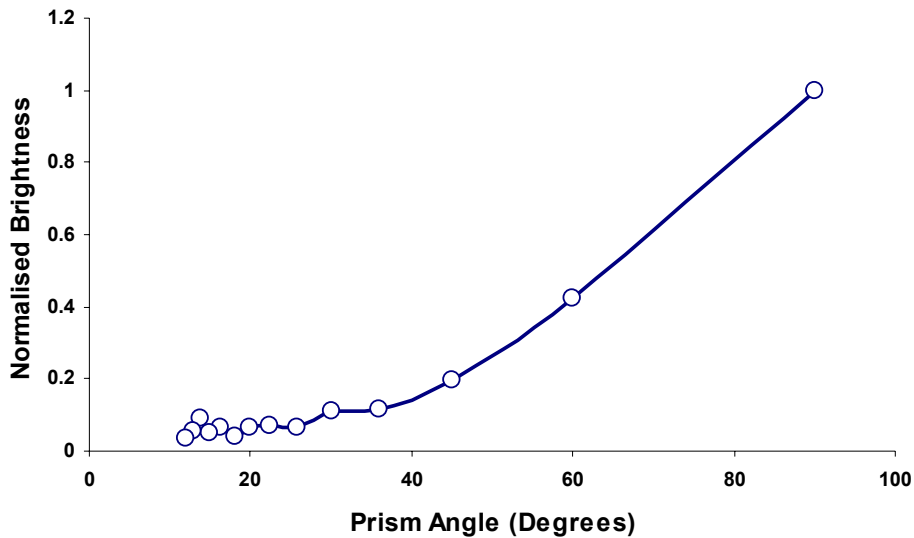


Figure 8: Laser brightness for those angles that generate petal patterns.

Because this resonator was modeled without any gain, the power content was determined as the inverse of the round trip losses after the mode has stabilized (therefore assuming that all the circulating power is deposited into the internal losses). It is also assumed that the output coupler of this system is not polarization dependent, which is sometimes the case, but not always. It is clear from the graph that the smaller the number of petal patterns, the higher the laser brightness.

#### 4. CONCLUSION

A model for a crossed Porro prism resonator that allows one to investigate all the output laser beam characteristics has been discussed. The model has been applied to the particular problem of output laser brightness from such resonators, where it has been shown that the brightness is strongly influenced by the angle between the two prism edges. At those angles at which petal patterns are observed, one finds an increase in the laser brightness relative to nearby non-petal pattern generating angles. There also appears to be a trend towards improved brightness and beam quality for those angles at which fewer petals are generated.

#### ACKNOWLEDGEMENTS

We would like to thank Denel Optronics for the use of their laser and for making experimental data available to us. We would also like to thank Dr Johan Steyl and Mr Gerhard Buchner for useful discussions on the subject of crossed porro prism resonators.

#### REFERENCES

1. G. Gould, S. Jacobs, P. Rabinowitz and T. Shultz., 1962. Crossed Roof Prism Interferometer, *Applied Optics* **1** (4), pp. 533 – 534.
2. I. Kuo and T. Ko., 1984. Laser resonators of a mirror and corner cube reflector: analysis by the imaging method, *Applied Optics* **23** (1), pp. 53 – 56.
3. G. Zhou and L.W. Casperson., 1981. Modes of a laser resonator with a retroreflecting roof mirror, *Applied Optics* **20** (20), pp. 3542 – 3546.
4. J. Lee and C. Leung., 1988. Beam pointing direction changes in a misaligned Porro prism resonator, *Applied Optics* **27** (13), pp. 2701 – 2707.
5. Y.A. Anan'ev, V.I. Kuprenyuk, V.V. Sergeev and V.E. Sherstobitov., 1977. Investigation of the properties of an unstable resonator using a dihedral corner reflector in a continuous-flow cw CO<sub>2</sub> laser, *Sov. J. Quantum Electron.*, **7** (7), pp. 822 – 824.
6. I. Singh, A. Kumar and O.P. Nijhawan., 1995. Design of a high-power Nd:YAG Q-switched laser cavity, *Applied Optics*, **34** (18), pp. 3349 – 3351.
7. N. Hodgson and H. Weber., 2005. *Laser Resonators and Beam Propagation* (2<sup>nd</sup> Ed.), Springer (New York), pp. 585 – 594.
8. Y.Z. Virnik, V.B. Gerasimov, A.L. Sivakov and Y.M. Treivish., 1987. Formation of fields in resonators with a composite mirror consisting of inverting elements, *Sov. J. Quantum Electron.*, **17** (8), pp. 1040 – 1043.
9. T.A. Anan'ev, 1973. Unstable prism resonators, **3** (1), pp. 58 – 59.
10. Litvin I.A., Burger L. and Forbes A., 2006. Physical optics modeling of modal patterns in a crossed Porro prism resonator, *accepted, GCL/HPL Symposium, Austria, September 2006*.
11. Litvin I.A., Burger L. and Forbes A., 2006. Porro prism resonators: a new approach, *in preparation*.
12. A.E. Siegman. 1990. New developments in laser resonators, *Proc. SPIE* **1224**, pp. 2 – 14.